Intracellular Silicon Chips in Living Cells**

Rodrigo Gómez-Martínez, Patricia Vázquez,* Marta Duch, Alejandro Muriano, Daniel Pinacho, Nuria Sanvicens, Francisco Sánchez-Baeza, Patricia Boya, Enrique J. de la Rosa, Jaume Esteve, Teresa Suárez,* and José A. Plaza**

Recent advances in microtechnology and nanotechnology have enabled microelectromechanical systems (MEMS) and nanoparticles to be used as interactive devices in cell biology.[1–6] Even though silicon MEMS, based on photolithographic processes, exhibit high performance and versatility[7] their use has been limited to extracellular applications, that is, cell biomolecular recognition,[8] manipulation,[9] mechanical analysis,[10,11] weighing,[12] and positioning.[13,14] In contrast, reported micro- and nanoparticles, characteristically formed or produced by chemical synthesis, have been used for intracellular applications.[15] Nowadays, progress in miniaturization of microelectronics and nanoelectromechanical systems (NEMS) technologies allows the fabrication of small silicon chips, a micrometer-size slice of a semiconductor material. Complex structures, smaller than cells, can be mass produced with nanometer precision in shape and dimensions and at low cost. Silicon, widely used by microelectronics industries, has been shown to have excellent electrical, mechanical, and chemical properties in many MEMS and NEMS. In addition, silicon chips can be chemically modified for molecular recognition.[16] Furthermore, many different materials (semiconductors, metals, and insulators) could be patterned on the silicon chip with accurate dimensions and geometries. In this Communication we investigate whether silicon-based intracellular chips (ICCs) with dimensions smaller than 3 μm can be produced and collected, internalized inside living cells, and used as intracellular sensors. We also investigate whether these small chips can be composed of more than one material and that can be nanostructured, allowing for the integration of electronic and mechanical parts at (ICC)-scale level, a key step for the production and use of innovative intracellular silicon-based micro- and nanochips.

First, we optimized the fabrication and collection of polysilicon chips smaller than 3 μm. Silicon-based microdevices were manufactured by combining photolithographic techniques with silicon microelectronic and micromachining technologies. This technology is based on the combination of a polysilicon device layer (0.5 μm) and a silicon oxide sacrificial layer coated (1.0 μm) onto a four-inch p-type silicon wafer ⟨100⟩ (Okmetic) (Figure 1A–C). The vertical dimensions of the chip are fixed with nanometer precision by the thickness of the device layer while photolithographic techniques define the micrometer or even submicrometric lateral dimensions. A 1.2-μm-thick HiPR 6512 photoresist (Fujifilm) layer was spun and irradiated (Karl-Süss MA6 contact aligner) through a chromium mask (Figure 1D). The irradiated area was dissolved and the chips were patterned by vertical polysilicon dry etching (Alcatel A601) using a modified Bosh process recipe (Figure 1E). The photoresist was removed by plasma etching (Tepla 300-E) and the chips were released by the etching of the silicon oxide sacrificial layer in vapors of hydrofluoric acid (HF) 49% (Figure 1F–H). Finally, the released chips (Figure 1I) were suspended by ultrasounds in ethanol for 5 minutes and the ICCs were collected by 5-μm filter rating (Hydrophilic PVDF, Millipore) and centrifuged at 1000 rpm for five minutes (MiniSpin Plus). This approach yielded more than 150 million devices for each four-inch wafer processed, all of controlled, precise, and reproducible shape and dimensions.

After testing different batches, polysilicon devices with lateral dimensions of 1.5–3 μm and with a thickness of 0.5 μm were selected to be placed inside living cells. We chose cells from the social organism *Dictyostelium discoideum* (*D. discoideum*) and human HeLa cells. We took advantage of the phagocytotic capacity of *D. discoideum* and incubated cells with ICCs at a ratio of 0.5–1 ICC/cell. Observation under optical light microscopy and

[*] R. Gómez-Martínez,[+] M. Duch, Prof. J. Esteve, Dr. J. A. Plaza[†]
Instituto de Microelectrónica de Barcelona
IMB-CNM (CSIC)
Campus UAB s/n
Cerdanyola, 08193 Barcelona (Spain)
E-mail: rodrigo.gomez@imb-cnm.csic.es
joseantonio.plaza@imb-cnm.csic.es
Dr. P. Vázquez,[+] Dr. P. Boya, Dr. E. J. de la Rosa, Dr. T. Suárez[†]
Centro de Investigaciones Biológicas, CIB (CSIC)
C/Ramiro de Maeztu 9, 28040 Madrid (Spain)
E-mail: pvazquez@cib.csic.es, teresa@cib.csic.es
A. Muriano, D. Pinacho, Dr. N. Sanvicens, Dr. F. Sánchez-Baeza
Instituto de Investigaciones Químicas y Ambientales de Barcelona
IIQAB (CSIC)
C/Jorge Girona, 18-26, 08034 Barcelona (Spain)
[+] R.G.-M. and P.V. contributed equally to this work.
[†] T.S. and J.A.P. are the project leaders.

[**] This study was financed by the Spanish government through the MINAHE 2 project MEC-TEC2005-07996-CO2-01, MINAHE 3 project MEC-TEC2008-06883-CO3-01, the health research project SAF2007-66175 (to EJdlR), and the INTRACELL project CSIC-200550F0241 8 (to JE, EJdlR & FSB). We acknowledge support (PV) from the CIBER de Diabetes y Enfermedades Metabólicas Asociadas (CIBERDEM). We want to thank Mayte Seisdedos, at the CIB, for her excellent assistance with confocal and time-lapse microscopy. We also thank the MEC-GICSERV program and the IMB-CNM clean-room staff.

Supporting Information is available on the WWW under http://www.small-journal.com or from the author.

DOI: 10.1002/smll.200901041

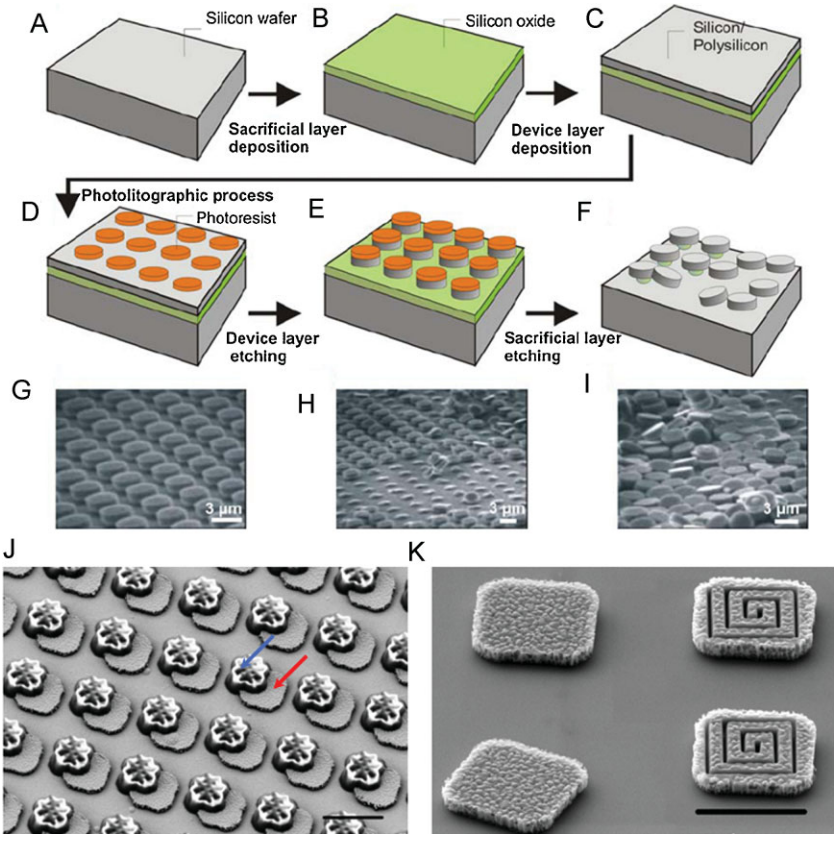

Figure 1. ICC fabrication process. A) Silicon wafer starting material. B) Silicon oxide (sacrificial layer) deposition. C) Polysilicon layer (device layer) deposition. D) Photoresist deposition and the photolithographic step. E) Device layer etching (chip pattering). F) Sacrificial etching and chip release. G–I) SEM images of ICCs after etching and vapors of the HF process. J) SEM images of ICCs of two misaligned materials: polysilicon square platform (red arrow) joined to a gold platform (blue arrow). K) SEM images of a 3 μm × 3 μm × 0.5 μm polysilicon ICC shown before (left) and after (right) a 3D coil nanostructuring by FIB nanomachining. Scale bar = 3 μm.

confocal laser scanning microscopy (CLSM) showed that ICCs were efficiently internalized by *D. discoideum* healthy cells (Figure 2A and C, and Supporting Information Figure S1A). Non-phagocytic cells such as HeLa cells, can internalize particles by endocytosis.[17] Preliminary experiments incubating HeLa cells with polysilicon ICCs (0.5–1 ICC/cell) gave low yields of internalized ICCs. We then used lipofection[18] (encapsulation of materials in a lipid vesicle called a liposome) to obtain higher rates of ICC-containing cells. After incubating liposomes containing polysilicon ICCs with HeLa cells, we observed a 50% increase in the number of ICC-containing cells, reaching an average of 25% and used lipofectamine hereafter. ICC internalization in HeLa cells was visualized by optical light microscopy and CLSM (Figure 2B and D and Supporting Information, Figure S1B). To confirm ICC internalization into the cytoplasm of HeLa cells we used a focused ion beam (FIB) station (Figure 2E–H).[19,20] This equipment allowed for the machining (with nanometer precision) of cells with internalized ICCs, and their high-resolution imaging by scanning electron microscopy (SEM).

To assess if the ICC-containing HeLa cells are healthy and alive after ICC internalization, we used the vital dye fluorescein diacetate (CFDA) and time-lapse microscopy. Interaction of CFDA with active intracellular esterases hydrolyzes the acetate groups, producing fluorescein emission, which can be observed under a fluorescent light. Alive ICC-containing HeLa cells display green fluorescence (Figures 2D and Supporting Information, Figure S1B). Time-lapse microscopy also showed healthy looking ICC-containing *D. discoideum* and HeLa cells (Supporting Information, Figures S2 and S3).

It has been recently reported that mesoporous silicon is biocompatible and biodegradable when used as an external multistage delivery system.[21] In the case of internalized polysilicon ICCs, we did not observe any toxic cellular response after 24 hours (see Supporting Information, Figures S2 and S3). To evaluate the effects of polysilicon ICCs on long-term cell viability, HeLa cells lipofected with ICCs were maintained for up to 7 days in proliferating cultures that resulted in confluent monolayers. After 3 and 7 days in culture, cell viability was assessed by loading HeLa cells with CFDA before fixation. Healthy living cells containing ICCs were observed 3 and 7 days after ICC lipofection (Supporting Information, Figure S4A and B). Cytotoxicity was further evaluated with propidium iodide (PI). Over 90% of cultured HeLa cells remained viable 7 days after lipofection and the same percentage of viable cells was observed for the ICC-containing HeLa cell population (Supporting Information, Figure S4C,D).

The use of engineered ICCs as intracellular sensors inside living cells constitutes a real challenge. After establishing that ICCs were not toxic to the cells, we derivatized ICCs with the same vital dye CFDA and delivered them to *D. discoideum* and HeLa cells. Functionalized ICCs inside *D. discoideum* and HeLa cells emitted green fluorescence, demonstrating that cells were alive and healthy one day after incubation with ICCs, as expected, and showing ICC interaction with intracellular esterases (Figure 3). CFDA-derivatized ICCs showed green fluorescence inside HeLa cells after 3 and 7 days in culture. This observation provides a proof of concept for measuring intracellular parameters.

Finally, to further demonstrate the technology versatility, we studied the integration of different materials in a single ICC and their nanostructuring capability. ICCs composed of 3 μm × 3 μm misaligned platforms of polysilicon and gold, respectively (Figure 1J), were fabricated by photolithographic processes, allowing precise dimensions and geometries of the two materials. In addition, it is also of fundamental importance that ICCs can be nanomachined in three dimensions using other common microelectronics techniques. For instance, a nanocoil on an ICC is defined by FIB milling (Figure 1K).

In conclusion, our results show that silicon-based top-down fabricated ICCs can be internalized by living eukaryotic cells

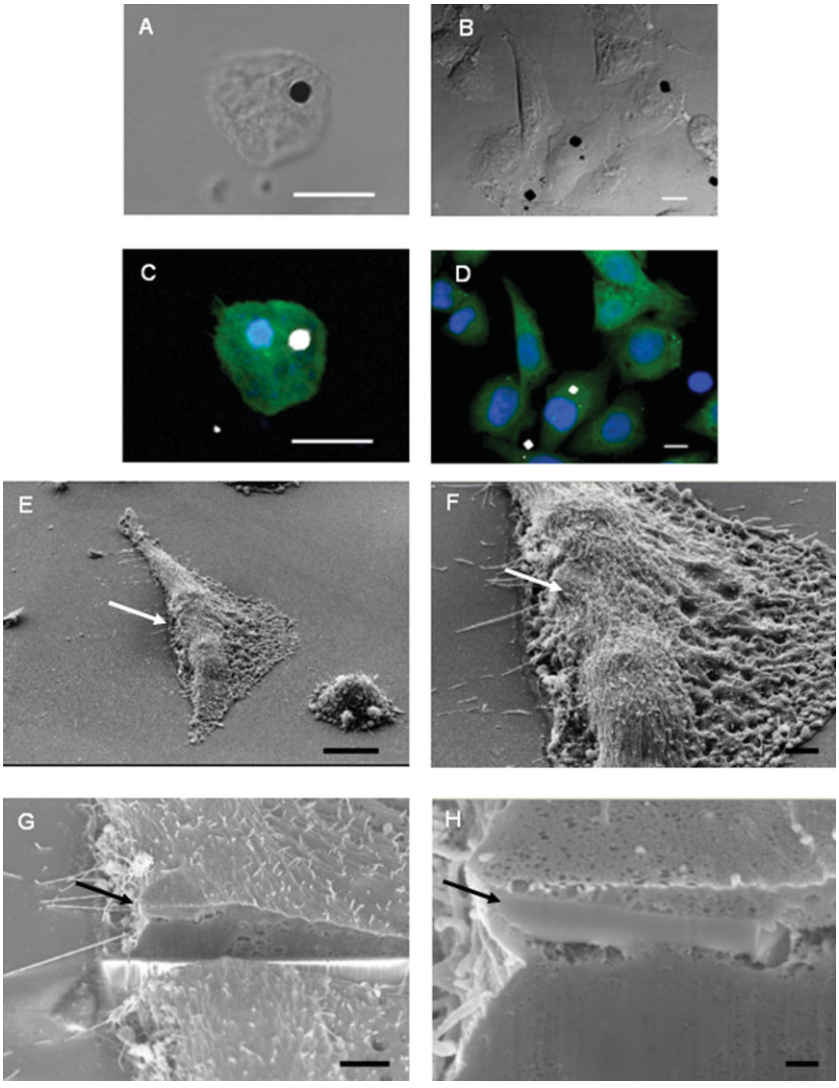

Figure 2. ICC internalization in eukaryotic cells. GFP-expressing *D. discoideum* (A,C) and HeLa cells loaded with the vital CFDA dye (B,D) show ICCs inside their cytoplasms. ICCs appear black in optical-light microscopy images (A,B) and in white in confocal laser images (C,D). SEM image of an ICC-containing HeLa cell (E,F). SEM image of a HeLa cell nanomachined by FIB where the ICC can be located inside the cell (G,H). Arrows indicate the position of the ICC. Scale bar in (A–E): 10 μm; (F,G) 3 μm; (H) 0.5 μm.

without interfering with cell viability, and functionalized ICCs could be used as intracellular sensors since they can interact with the cell cytoplasm. ICCs have similar dimensions to many synthesized micro- and nanoparticles but they have the advantages of silicon-chip technology. ICCs offer higher flexibility and versatility in shape and size and they can be nanostructured in three dimensions and integrated with several materials (semiconductors, insulators, metals) at chip-scale level. Nowadays, there is huge interest in biophysical single-cell properties. Consequently, compared to synthesized nanoparticles, silicon-based nanostructured devices can address the measurement of intracellular mechanical properties. We believe that our present work makes important progress towards functional intracellular NEMS. The challenge for further research will be miniaturization of electromechanical devices in combination with cytotoxicity studies for each specific device and cell lines. In the near future, silicon-based micro- and nanodevices will permit the characterization, quantification, and in vivo real-time monitoring of cellular events inside a single cell.

Experimental Section

Cell manipulation: D. discoideum cells constitutively expressing green fluorescent protein (GFP) or wild-type cells were seeded in 24-well dishes (65000 cells/well) and kept in starvation (2 h at 25 °C) to induce phagocytosis. Cells were then incubated in the presence of polysilicon ICCs (2 h at room temperature (RT); 0.5–1 ICCs/cell). For experiments in the human HeLa cell line, ICCs were first mixed (0.5–1 ICCs/cell) with Lipofectamine 2000 (Invitrogen, Carlsbad, Ca, EE.UU.). HeLa cells were plated in 24-well dishes (25000 cells/well), incubated with ICC-containing liposomes and cultured in standard conditions for 1, 3, and 7 days. Cell viability was analyzed by incubating cells with Cell Tracker Green 5-cloromethyl fluorescein diacetate (CFDA; Molecular Probes, Invitrogen) for 15 min at 37 °C. *D. discoideum* and lipofected HeLa cells were fixed with 4% paraformaldehyde in PBS for 45 min. The nuclei were stained with DAPI for 10 min (4′,6′-diamino-2-phenylindole; Molecular Probes) and the cells were mounted with Fluoromont-G (Southern Biotech, Alabama, USA) for standard microscopy. HeLa cells were incubated with propidium iodide (PI, 1 μg mL^{-1}), commonly used to identify dead cells. Cells were counted immediately after the incubation. Living cells do not uptake PI.

Cell imaging: To localize internalized ICCs, a TCS SP2 AOBS confocal laser scanning microscope with 63 × oil immersion lens (Leica, Heidelberg, Germany) was used. *D. discoideum* cells constitutively expressing GFP and HeLa cells treated with CFDA were monitored with excitation and emission settings of 488 nm and 505–550 nm, respectively. A 351-nm laser line was used to image nuclei and fluorescence emission was measured at 415–460 nm. Polysilicon ICCs were imaged with a 488-nm laser line and they were detected by reflected light at 480–495 nm. Before SEM examination, HeLa cells were fixed with 2.5% glutaraldehyde in a sodium cacodylate 0.1 M pH 7.4 solution at RT, dehydrated in an ethanol series, critical point-dried using CO_2 (K850 critical point drier Emitech), mounted on the specimen holder, coated with gold and observed in an S-570 SEM (Hitachi. Tokyo, Japan). Cells were sectioned by the FIB beam to visualize ICCs using a combined Strata 235 dual-beam FIB and SEM work station (FEI. Hillsboro, OR, USA). Time- lapse microscopy was performed with a Leica AF6000 LX model DMI6000B *D. discoideum* and HeLa

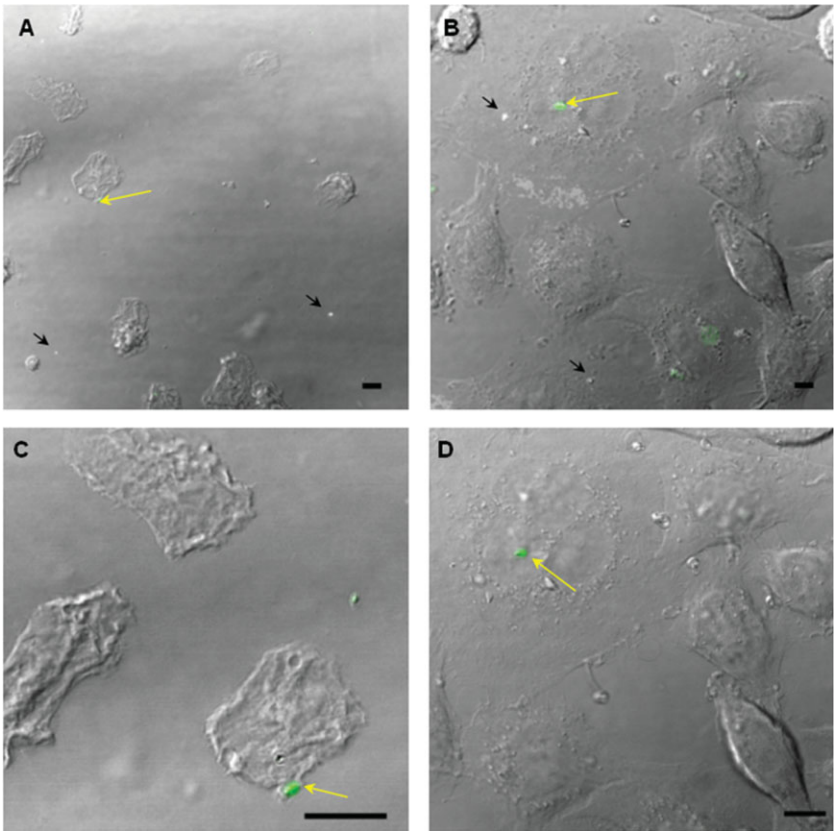

Figure 3. CFDA-derivatized ICCs interact with the cell cytoplasm. *D. discoideum* (A, C) and HeLa cells (B, D) show intracellular ICCs with green fluorescence (yellow arrow). Extracellular ICCs do not display fluorescence and appear as white dots (black arrow) (A, B). Zoom of *D. discoideum* (C) and HeLa cells (D) showing functionalized ICCs. Images are maximal confocal projections taken with CLSM. Bar = 10 μm.

cells films were made with pictures taken every 30 s and 15 min, respectively.

Chip derivation: ICCs were cleaned with HNO3/MeOH (3:7), dimethylformamide (DMF):milliQ H_2O (7:3, 3 × 1 mL) and with ethanol (3 × 1 mL). To activate their surface, ICCs were incubated in a 1% KOH/ethanol solution (10 min), washed with DMF:milliQ H2O (7:3, 3 × 1 mL) and with anhydrous ethanol (3 × 1 mL). Surface amination was achieved by incubation in 2.5% (v/v) 3-aminopropyl-trimethoxy silane (3 h/RT) followed by washing with anhydrous ethanol (3 × 1 mL) and with anhydrous DMF (3 × 1 mL). A 1 mM solution of fluorescein diacetate isothiocyanate in anhydrous DMF was added and the chips were left to react for 12 h at RT in the dark. Finally, ICCs were washed with anhydrous DMF (3 × 1 mL) and stored in methyl tert-butyl ether. The solvents used were filtered with 0.45-μm filters and centrifugations were carried out for 10 min at 1500 g (10 °C).

Keywords:

biosensors · cells · microtechnology · nanoparticles · silicon chips

[1] M. Ferrari, *Nat. Rev. Cancer.* **2005**, *5*, 161–171.
[2] G. A. Silva, *Nat. Rev. Neurosci.* **2006**, *7*, 65–74.
[3] H. Andersson, A. Van den Berg, *Curr. Opin. Biotechnol.* **2004**, *15*, 44–49.
[4] L. Bousse, *Sens. Actuators, B.* **1996**, *34*, 270–275.
[5] G. M. Whitesides, *Nat. Biotechnol.* **2003**, *21*, 1161–1165.
[6] D. B. Weibel, W. R. DiLucio, G. M. Whitesides, *Nat. Rev. Microbiol.* **2007**, *5*, 209–218.
[7] J. Voldman, *Nat. Mater.* **2003**, *2*, 433–434.
[8] G. Shekhawat, S. H. Tark, V. P. Dravid, *Science* **2006**, *311*, 1592–1595.
[9] C. C. Striemer, T. R. Gaborski, J. L. McGrath, P. M. Fauchet, *Nature* **2007**, *445*, 749–753.
[10] G. Bao, S. Suresh, *Nat. Mater.* **2003**, *2*, 715–725.
[11] S. E. Cross, Y. S. Jin, J. Rao, J. K. Gimzewski, *Nat. Nanotechnol.* **2007**, *2*, 780–783.
[12] T. P. Burg, M. Godin, S. M. Knudsen, W. Shen, G. Carlson, J. S. Foster, K. Babcock, S. R. Manalis, *Nature* **2007**, *446*, 1066–1069.
[13] H. Lee, Y. Liu, D. Ham, R. M. Westervelt, *Lab Chip* **2007**, *7*, 331–337.
[14] D. S. Gray, J. L. Tan, J. Voldman, C. S. Chen, *Biosens. Bioelectron.* **2004**, *19*, 1765–1774.
[15] S. K. Murthy, *Int. J. Nanomed.* **2007**, *2*, 129–141.
[16] J. Fritz, M. K. Baller, H. P. Lang, H. Rothuizen, P. Vettiger, E. Meyer, H.-J. Güntherodt, Ch. Gerber, J. K. Gimzewskj, *Science* **2000**, *288*, 316–318.
[17] S. E. A. Gratton, P. A. Ropp, P. D. Pohlhaus, J. C. Luft, V. J. Madden, M. E. Napier, J. M. De Simone, *Proc. Natl. Acad. Sci. USA* **2008**, *105*, 11613–11618.
[18] V. Ciccarone, Y. Chu, K. J. P. Pichet, P. Hawley-Nelson, K. Evans, L. Roy, S. Bennett, *Focus* **1999**, *21*, 45–55.
[19] M. Milani, M. Ballerini, D. Batani, F. Squadrini, F. Cotelli, C. Lora Lamia Donin, G. Poletti, A. Pozzi, K. Eidmann, A. Stead, G. Lucchini, *Eur. Phys. J. Appl. Phys.* **2004**, *26*, 123–131.
[20] D. Drobne, M. Milani, A. Zrimec, V. Leser, M. Berden, *J. Microscopy.* **2005**, *219*, 29–35.
[21] E. Tasciotti, X. Liu, R. Bhavane, K. Plant, A. D. Leonard, B. K. Price, M. M.-C. Cheng, P. Decuzzi, J. M. Tour, F. Robertson, Ferrari. Mauro, *Nat. Nanotechnol.* **2008**, *3*, 151–157.

Received: June 16, 2009
Published online: December 21, 2009